ACS APPLIED MATERIALS & INTERFACES

Research Article

www.acsami.org

Preparation and Characterization of Polyhedral Oligomeric Silsesquioxane-Containing, Titania-Thiol-Ene Composite Photocatalytic Coatings, Emphasizing the Hydrophobic–Hydrophilic Transition

LaCrissia U. Jefferson,[†] Anton D. Netchaev,[‡] Jennifer A. Jefcoat,[†] Amber D. Windham,[†] Frederick M. McFarland,[†] Song Guo,[†] Randy K. Buchanan,[‡] and J. Paige Buchanan*,[†]

[†]Department of Chemistry and Biochemistry and [‡]School of Computing, University of Southern Mississippi, Hattiesburg, Mississippi 39406, United States

Supporting Information

ABSTRACT: Coatings prepared from titania-thiol-ene compositions were found to be both self-cleaning, as measured by changes in water contact angle, and photocatalytic toward the degradation of an organic dye. Stable titania-thiol-ene dispersions at approximately 2 wt % solids were prepared using a combination of high-shear mixing and sonication in acetone solvent from photocatalytic titania, trisilanol isobutyl polyhedral oligomeric silsesquioxane (POSS) dispersant, and select thiol-ene monomers, i.e., trimethylolpropane tris(3-mercaptopropionate) (TMPMP), pentaerythritol allyl ether (APE), and 1,3,5-triallyl-1,3,5-triazine-2,4,6(1*H*,3*H*,5*H*)-trione (TTT). The dispersed particle compositions were characterized by DLS and TEM. The synthetic methods employed yield a strongly bound particle/POSS complex, supported by IR, ^{29}Si NMR, and TGA. The factors of spray techniques, carrier solvent volatility, and particle size and size distributions, in combination, likely all contribute to the highly textured but uniform surfaces observed via SEM and AFM. Polymer composites possessed thermal transitions (e.g., T_g) consistent with composition. In general, the presence of polymer matrix provided mechanical integrity, without significantly compromising or prohibiting other critical performance characteristics, such as film processing, photocatalytic degradation of adsorbed contaminants, and the hydrophobic–hydrophilic transition. In all cases, coatings containing photocatalytic titania were converted from superhydrophobic to superhydrophilic, as defined by changes in the water contact angle. The superhydrophilic state of samples was considered persistent, since long time durations in complete darkness were required to observe any significant hydrophobic return. In a preliminary demonstration, the photocatalytic activity of prepared coatings was confirmed through the degradation of crystal violet dye. This work demonstrates that a scalable process can be found to prepare titania-thiol-ene coatings having improved coating properties which also exhibit photocatalytic and self-cleaning attributes.

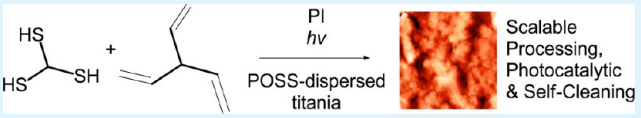

KEYWORDS: *photocatalytic, thiol-ene, coatings, titanium dioxide, polyhedral oligomeric silsesquioxane*

1. INTRODUCTION

In the presence of light, water, and oxygen, the surface of anatase titania (TiO_2) may be activated, thereby creating a surface that is both photocatalytic and has undergone changes in surface energy described as a hydrophobic–hydrophilic switching mechanism.[1,2] The transition from the hydrophobic to hydrophilic state allows for the preparation of self-cleaning surfaces, which have numerous potential applications in air and water purification and in the cleaning and maintenance of infrastructure.[3,4] Additional metal oxide semiconductors, such as $NaTaO_3$, $SrTiO_3$, and Cr or Sb doped TiO_2, have been explored for their self-cleaning characteristics.[5] However, in an overall comparison of toxicity, stability, activity, and cost, titania has been credited as the prominent photocatalyst in the self-cleaning arena.[6] As introduced, the photocatalytic activity of titania-containing thin films may be described by these two synergistic events: a photocatalytic pathway based on a series of redox reactions leading to the degradation of adsorbed organic contaminants and a photoinduced switching between hydrophobic–hydrophilic states of the coated surface inducing self-cleaning attributes.[7] These surface changes occur following absorption of light of specific wavelengths characteristic of the band gap energy of the photocatalyst (~3.2 eV or ~380 nm, for undoped TiO_2), where surface electron–hole (e^-/h^+) pairs are generated and promote the production of free radicals and super oxides. These powerful reactive species scavenge the coated surface for organic material, which is ultimately converted into carbon dioxide and water, provided that complete oxidation occurs.[8] As a result, the application of photocatalytic materials for environmental remediation, where the process includes light, generally low-cost photocatalysts in primarily aqueous environments, and where carbon dioxide and

Received: July 9, 2014
Accepted: May 22, 2015
Published: May 22, 2015

DOI: 10.1021/acsami.5b01488
ACS Appl. Mater. Interfaces 2015, 7, 12639–12648

water are the primary reaction products, has received worldwide attention.[9,10]

The accepted mechanism of the hydrophobic−hydrophilic transition includes the generation of oxygen vacancies during activation of the titania surface, permitting water molecules to bind to these defect sites.[11] As the density of water molecules bound to the surface increases, a redistribution of the hydrogen bonds of water molecule clusters ensues, and the surface increases in hydrophilicity.[12,13] In the hydrophilic state, the interaction energy between a water droplet and the surface is stronger than the cohesive forces of bulk water causing the droplet to spread out versus bead up on surface contact.[14−16] In this process, any fouling of the surface is simply washed away, also known as self-cleaning. Miyauchi et al.[17] determined that a substrate may remain in the hydrophilic state until the surface-bound hydroxyl groups are removed.

Historically, the ability to make high-performance photocatalytic coatings using dispersed titania depends heavily on dispersion stability. Without a dispersing aid, titania will quickly form large aggregates and precipitate from the dispersion. As a result, there is a persistent effort to find dispersing aids to increase the shelf life stability, reduce the number and size of aggregates, and produce a composition which can be readily applied to a substrate as a coating.[18] Common methods of dispersing particles are electrostatic repulsion and steric stabilization. Electrostatic repulsion is common in aqueous dispersions of titania, where either a modulation of the pH of the continuous phase relative to the isoelectric point of titania results in a charged particle surface or through the addition of charged polyelectrolytes.[19] Steric stabilization is entropically driven and may include the use of neutral or charged species as dispersants or as chemically grafted moieties; moreover, this approach is more amenable to dispersed particles in organic media. Hybrid molecules such as polyhedral oligomeric silsesquioxanes (POSS), possessing both inorganic and organic attributes, may be employed as dispersants and can be synthetically designed for aqueous and nonaqueous formulations.[20−23] The amphiphilic nature, steric bulk, cage-preorganization, and presence of reactive groups all contribute to POSS's success as a particle dispersant.[24−26]Trisilanol isobutyl POSS molecules, Figure 1, possess isobutyl groups on the cage-like structure to provide steric stabilization and organic solvent compatibility. Simultaneously, the three silanol groups (Si−OH) can associate with the dispersed particles via covalent and noncovalent bonding interactions creating a high-surface-area structure.[27,28]Bond-forming condensation reactions with surface Ti−OH groups produce covalent linkages, while hydrogen bonding and dipole−dipole interactions among polar groups, although noncovalent, are also significant.[29]

Our group desires to produce stable titania dispersions suitable for spray-coating which are characterized by excellent coating properties and photocatalytic activity, both in the hydrophobic−hydrophilic transition and in the photodegradation of organic surface contaminants. The coating would eventually be applied as a high-performance top-coat, potentially for retrofitting of common infrastructures. To provide the fundamental physical coating characteristics, such as adhesion, a thiol-ene matrix was chosen. The thiol-ene reaction is based on a free-radical, step-growth polymerization mechanism.[30] The reaction's selectivity, high monomer conversions, insensitivity to molecular oxygen, and few competing reactions are many of the reasons for the popularity of this thiol-ene "click" reaction.[31,32] A large number of

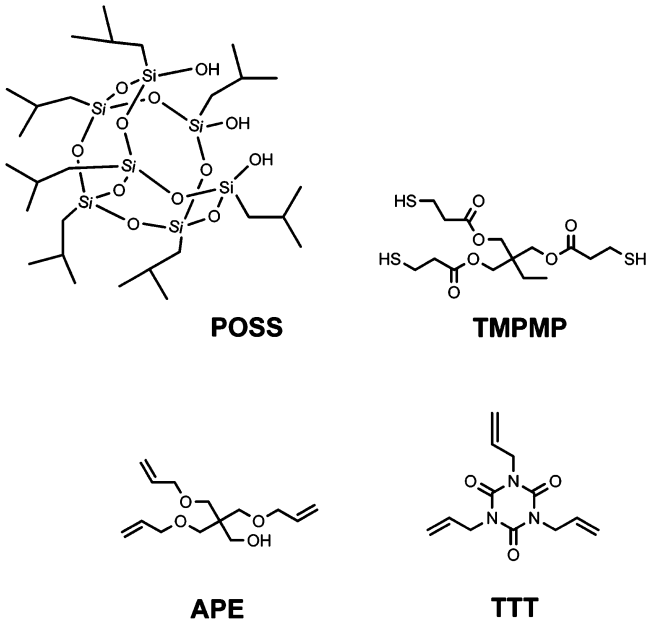

Figure 1. Chemical structures of the dispersant and monomers used in formulations: trisilanol isobutyl polyhedral oligomeric silsesquioxane (POSS); trimethylolpropane tris(3-mercaptopropionate) (TMPMP); pentaerythritol allyl ether (APE); 1,3,5-triallyl-1,3,5-triazine-2,4,6-(1*H*,3*H*,5*H*)-trione (TTT).

commercially available thiols and enes permits the tailoring of polymer network properties for a variety of applications.[33] The attractive polymerization rates and uniform polymer networks produced make the thiol-ene matrix an ideal choice for polymer−particle composite coatings.[31−33] One recent example from our group is the incorporation of gold nanoparticles into photocured thiol-ene matrices to produce optically clear antistat coatings for electronic components.[34] Additional systems explored by Hoyle et al.[31,32] included fundamental ways to incorporate POSS and silica as coating constituents of thiol-ene networks.

The primary goal of the research effort described herein is the synthesis and preliminary characterization of POSS-containing, titania-thiol-ene composite coatings. Of particular interest is the effect of dispersant and matrix components on coatings performance, such as the hydrophobic−hydrophilic transition and the related photocatalytic activity. Prepared dispersions and the resulting composite coatings are characterized using a variety of standard techniques as a function of irradiation wavelength, time, and composition. During this effort, a custom photoreactor was assembled to facilitate environmental control of samples during treatments. This work is a representative effort of our larger mission to advance the application of thiol-ene polymerizations to the preparation of novel particle−polymer composites.

2. EXPERIMENTAL SECTION

2.1. Materials. Powder particles of titania (VP Aeroperl P25/20, titanium(IV) oxide/anatase) with vendor reported average particle sizes of 20 μm and 25 nm were obtained from Evonik and Sigma-Aldrich, respectively. Nanopowder silica particles (10−20 nm) were also obtained from Sigma-Aldrich and used as a reference non-photocatalytic material. The free-flowing white powder trisilanol isobutyl polyhedral oligomeric silsesquioxane (SO1450, POSS) was obtained from Hybrid Plastics, Hattiesburg, MS. The solvent, acetone (99.5%), trimethylolpropane tris(3-mercaptopropionate) (TMPMP,

DOI: 10.1021/acsami.5b01488
ACS Appl. Mater. Interfaces 2015, 7, 12639−12648

96−99%), pentaerythritol allyl ether (APE, 70%; remaining 30%, monoene), and 1,3,5-triallyl-1,3,5-triazine-2,4,6(1*H*,3*H*,5*H*)-trione (TTT, 98%), was purchased from Sigma-Aldrich. All samples were used as received.

2.2. Dispersion Preparation and Characterization. The titania and POSS compositions were held constant at 10:1 wt/wt % in the following procedure. Using a Flacktek speed mixer, titania and POSS solids were combined and placed under high sheer for 5 min. Acetone was added to the solids to achieve a 5 wt % solids dispersion. With a combination of the speed mixer and a Fisher Scientific Model FS110 FS 20 sonicator, the dispersion was alternatively placed under high shear with glass beads (diameter 3−4 mm) followed by sonication in 5 min increments each for three cycles. Monomers were added to the dispersion and speed mixed for an additional 5 min. Glass beads were mechanically removed prior to the transfer of the dispersion to the sprayer.

Dynamic light scattering (DLS) analysis was conducted using a Microtrac instrumentation suite, including Zetatrac and S3500 models. The titania particles were treated as irregular shaped with a refractive index of 2.55 (anatase titania). A refractive index of 1.36 and a dielectric constant of 21.0 were used for acetone in these measurements. Particle sizes were obtained on the dispersions. Particle sizes were reported as volume average (MV) distributions, where MV is more sensitive to the presence of a larger molecular weight fraction.

2.3. Physical and Chemical Characterization of Dispersions. Dispersions were characterized using thermal and chemical analysis techniques. Thermal characterization was obtained via thermogravimetric analysis (TGA) using a TA Instruments Q500. Samples of approximately 5−10 mg were evaluated in platinum pans over the temperature range 0−800 °C with a heating rate of 20 °C/min under a nitrogen atmosphere. Fourier transform infrared spectroscopy (FTIR) was used to identify the changes in chemical bonding of dispersed particles. Spectra were acquired in the 4000−400 cm^{-1} range with a Nicolet 6700 FTIR spectrophotometer using an ATR accessory (diamond crystal). Small aliquots of the dispersions were applied to Formvar carbon film on 300 mesh copper grids, purchased from Electron Microscopy Sciences, and the solvent was removed by evaporation. Images were acquired on a Zeiss EM-900 transmission electron microscope (TEM), operated at 50 kV and magnifications of 140 000×. Solid state ^{29}Si NMR data was obtained at a frequency of 79.5 MHz using a Bruker MSL-400 NMR spectrometer equipped with a CP/MAS double air bearing probe. Ground samples were packed in 4 mm fused zirconia rotors and sealed with Kel-FTM caps. All chemical shifts were referenced to the downfield peak of tetrakis-(trimethylsily1)silane (−9.8 ppm with respect to TMS).

2.4. Coating Preparation and Characterization. The dispersions were transferred to an Iwata Eclipse Gravity Feed Airbrush-CS-Size: 0.35 mm/Testors Blue Mini Airbrush with compressor, adding IRGACURE 651 at 1 wt % monomers. The substrates, aluminum Q-panels (3 in. × 6 in.), glass microscope slides (3 × 1 × 1.0 mm^3), silicon wafer chips, and glass slides were sprayed with the dispersions in an interlaced spray-pattern at a distance of 30 cm. A horizontal pass plus one vertical pass over the substrate is considered one coat, and a total of 10 coats were applied. Coatings were dried between each coat in a Fisher Isotemp oven at 50 °C for 2 min, producing thin 3−5 μm coatings. Alternatively, dispersions were cast in Teflon molds to permit easy removal for DSC analysis; thickness of cast samples ranged 100−200 μm. All coatings were stored in a desiccator at ∼2% RH followed by UV curing for 90 min at 350 nm, unless otherwise noted. Substrates varied according to the experimental protocols, aluminum for contact angle and adhesion, silicon wafers (Ted Pella, Inc.) for scanning electron microscopy, and glass for crystal violet degradation studies. The crystal violet dye (3.5 g/L) was applied to the titania coating on glass and stored in a dark desiccator prior to use. An FEI Quanta 200 environmental scanning electron microscope (ESEM) and an NT-MDT Vita atomic force microscope (AFM) were employed in the analysis of the surface topology of prepared films. Images at various magnifications were obtained and recorded. The TA Instruments modulated differential scanning calorimeter (DSC) Q2000 instrument was used to monitor the samples over the temperature range −50 to 50 °C in a heat/cool/heat cycle at 3 °C/min. T_g information was taken from the second heating cycle.

2.5. Photochemical Studies and UV Treatment. A photoreactor chamber was constructed to easily facilitate environmental control of samples (temperature, purge gas, and relative humidity) and increase user safety (light exposure) during irradiation. A more detailed description and images of the photochemical chamber are provided in the Supporting Information, Figures S1−S3. The unit is equipped with a sealed aluminum sample holder with a quartz window, connectors for 5 UV lamps, an exhaust fan, and power controls. Relative humidity (RH) of the sample holder purge flow is measured with an installed capacitance-based 10−95% relative humidity range sensor. Temperature is measured via a type K thermocouple with a range −200 to +1250 °C. Coating interrogation for surface studies was conducted at 313 and 350 nm at a constant temperature of 25 °C and RH of 31 ± 2%, respectively.

2.6. Surface Analysis through Water Contact Angle. The relative surface energy characteristics of the prepared coatings were observed via water contact angle measurements. Changes in contact angle were monitored at 25 °C using a VCA 2500-AST goniometer, equipped with a light source, camera, and flat horizontal support for sample substrates. Typical water drops of 5 μL were deposited on the substrate, and the static contact angle between the spreading front edge and the substrate was calculated. Both sides of the drop were included, and five drops were applied to the substrate for a total of 10 contact angle measurements per data point.

3. RESULTS AND DISCUSSION

Since the hydrophobic−hydrophilic transition is primarily a surface phenomenon, the physical and chemical attributes of the surface are of paramount importance.[1,7,35−47] Reported surface characteristics of coated samples and their resulting photocatalytic activity are linked to the quality of the dispersions from which they are prepared. This relationship between particle size, size distribution, film preparation method, and other film characteristics such as self-cleaning activity must be defined experimentally, since the packing of the particles into the solid state and the resulting film topology is heavily dependent on these variables. Our current study probes the hydrophobic−hydrophilic transition of sprayed films prepared from a combination of titania particles (micron, M and nanoscale, N) and a POSS derivative as dispersant, with select thiol and ene monomers for polymerization, Figure 1. Compositions prepared during this study are provided in Table 1 with brief descriptions. Both common constituents of thiol-ene coatings, APE and TTT, were selected to explore structure−property relationships.[31] In general, 2 wt % acetone

Table 1. Compositions of POSS-Containing, Thiol-Ene Composite Samples Prepared from the Dispersant and Monomers Illustrated in Figure 1

dispersed particle, no monomers[a]	dispersed particle, thiol (TMPMP), and ene (APE)[b]	dispersed particle, thiol (TMPMP), and ene (TTT)[b]
M	M/TMPMP/APE	M/TMPMP/TTT
N	N/TMPMP/APE	N/TMPMP/TTT
S	S/TMPMP/APE	S/TMPMP/TTT

[a]Film control samples were prepared from dispersed particles (1.6 wt %) containing POSS (0.2 wt %), without monomers. [b]Composite components were mixed in acetone solvent to achieve a final composition of particle, M, N,or S (1.6 wt %); POSS (0.2 wt %); and total monomer, thiol + ene in 1:1 mol equiv (0.2 wt %); all coatings were prepared from dilute dispersions by spray-coating.

DOI: 10.1021/acsami.5b01488
ACS Appl. Mater. Interfaces 2015, 7, 12639−12648

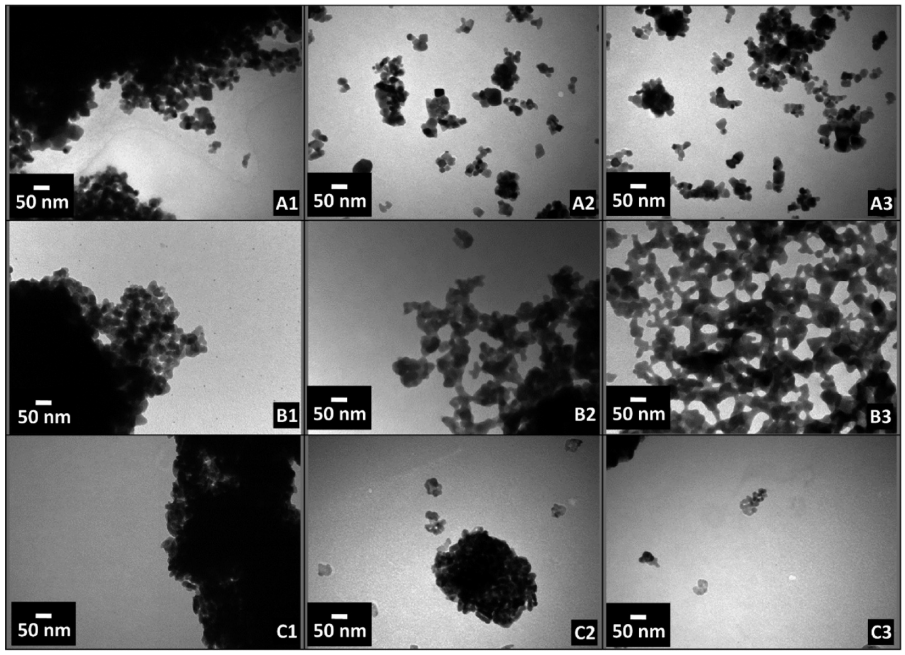

Figure 2. TEM images of dispersed particles and composite samples prior to coating application, left to right: A1 = pure particle, no dispersants or monomers; A2 = M, dispersed particle, no monomer; A3 = M/TMPMP/TTT, composite dispersion; followed by the analogous silica S (B1−B3) and nanoscale titania N (C1−C3) series.

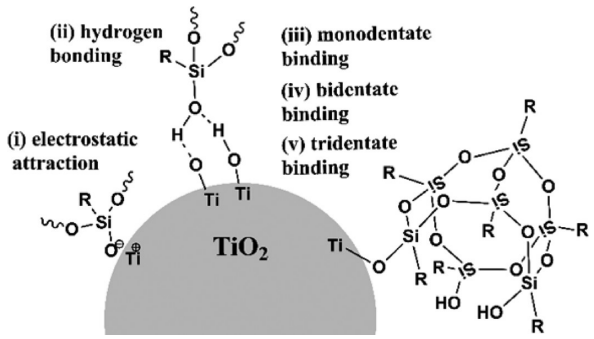

Figure 3. Potential binding states of dispersed particles via the silanol groups of POSS: (i) electrostatic attraction, (ii) hydrogen bonding, (iii) monodentate binding, (iv) bidentate binding, and (v) tridentate binding.

dispersions, suitable for spray-coating, contained titania (1.6 wt %), dispersant (0.2 wt %), and thiol-ene monomers (0.2 wt %), and this combination produced dispersions having long-term stability, with a representative sample in Supporting Information Figure S4. The presence of the POSS dispersant was found to be critical to dispersion stability. Dispersions were also prepared from silica particles (S), using the same combinations and concentrations of dispersants and monomers, to allow a direct comparison to a nonphotoactive material.

DLS and TEM techniques were combined to probe the effects of particle size and size distributions of the dispersions in the presence of the POSS dispersant and the thiol-ene monomers used for polymerization, but prior to actual film preparation. An initial concern was that, by adding organic monomers to the prepared dispersions, an onset of agglomeration would be observed. The particle size and particle size distributions of prepared dispersions fluctuated over the sample series, in their respective ranges (micron versus nano, for example), but were not increased by the addition of monomers. For example, N and S dispersions exhibited an expected decrease in average particle size from 0.7 and 1.1 μm to 0.2 and 0.1 μm, respectively, after the addition of dispersants, which did not increase after the addition of monomer. Raw DLS data can be found in Supporting Information, Table S1. In general, TEM data is consistent with DLS; however, it identifies the presence of larger aggregates in the N samples, Figure 2, which becomes important in film preparation. Overall, the addition of monomers does not promote agglomeration in the dispersion, and samples retain the long term stability required for film preparation.

The POSS dispersant chosen for this study contains three silanol functionalities, which leads to a number of different theoretical bonding interactions between the particle and POSS, Figure 3. These potential bonding states include the noncovalent electrostatic interactions of charged functional groups and the hydrogen bonding made possible among the OH groups presenting at the particle surface and POSS. Different binding motifs, monodentate, bidentate, and tridentate-like binding, resulting from covalent bonds between the particle and POSS silanols are also likely. Prior to dispersion in solvent, titania and POSS solids are mixed under high shear, where a significant increase in temperature of the post-sheared samples is noted. Enhancement of the bonding strength between particle and POSS was anticipated through thermally driven condensation reactions of POSS silanols (Si−O−H) with surface titanols (Ti−O−H).

Using previously published methods as a guide,[29,48] a combination of IR, ^{29}Si NMR, and TGA techniques were employed to ascertain the extent of bonding interaction between the particle and POSS in the dispersed phase. The presence of new chemical bonds was probed using IR spectra, Supporting Information Figure S5, obtained on the POSS-treated particle samples (M, N, and S) when compared to the pure materials. Titania, silica, and POSS present characteristic spectra, including the Ti−O−Ti at 480 cm^{-1}, isobutyl groups

DOI: 10.1021/acsami.5b01488
ACS Appl. Mater. Interfaces 2015, 7, 12639−12648

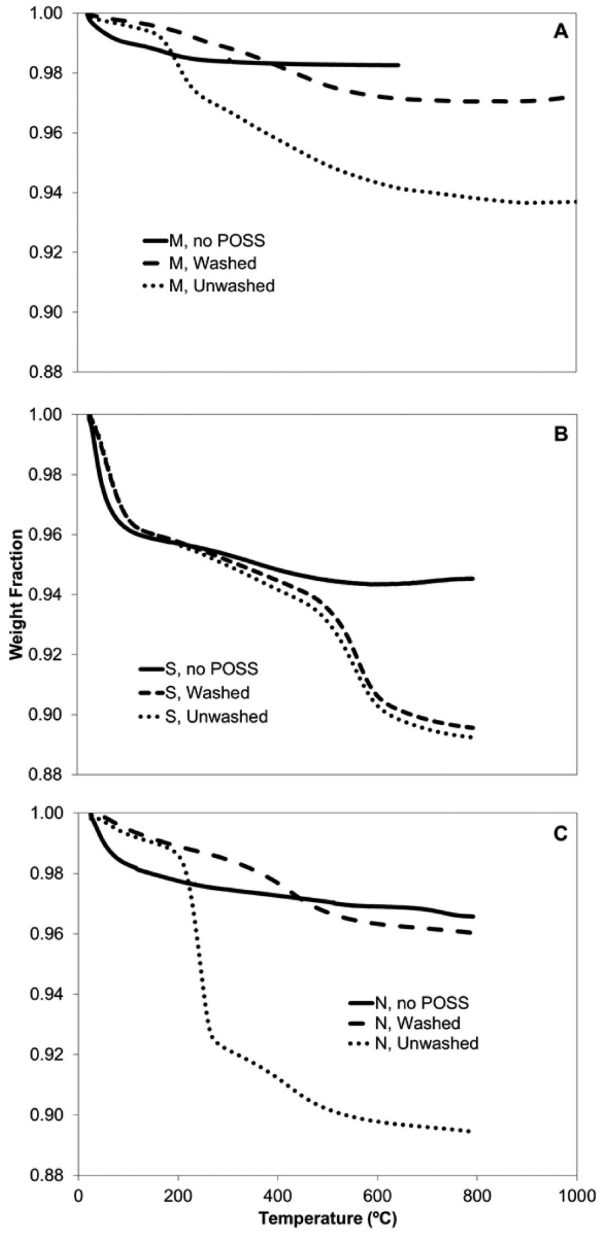

Figure 4. TGA analysis of POSS-treated powder samples before (unwashed) and after (washed) washing with hexane solvent: (A) micron titania particle series, M; (B) silica, S; and (C) nanotitania, N. Pure particle samples, prior to modification with POSS, are provided for comparison.

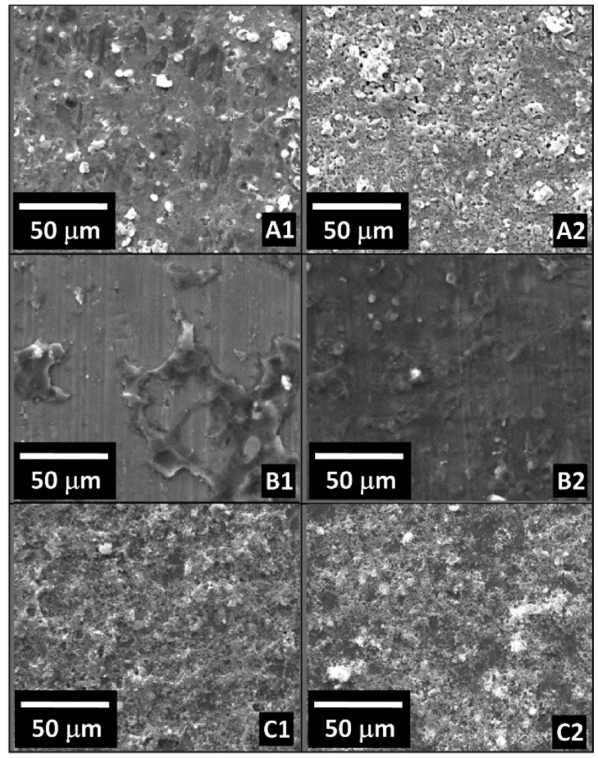

Figure 5. Representative SEM images of coating area residing inside the crosshatch, post-adhesion-test via ASTM D3359, for dispersed particles and composite coatings: (A1) M; (A2) M/TMPMP/TTT; (B1) S; (B2) S/TMPMP/TTT; (C1) N; (C2) N/TMPMP/TTT.

CH (2952 cm^{-1}), CH_3 (2867 cm^{-1}), and the indicative silicate and silanols at 1081 and 1227 cm^{-1}. The modified titania composite samples exhibit the expected characteristics of both starting materials; however, a shift and reduction in the silanol band (1097 cm^{-1}) is observed due to the interfacial binding occurring at the titania surface. In samples prepared from silica, S series, Si−OH and Si−O−Si bonds are prevalent in both starting materials and composites, yielding little information in the composite IRs. Solid state ^{29}Si NMR, Supporting Information Figure S6, was employed as a second means to support the changes in POSS silanols upon thermal treatment with titania. The ^{29}Si NMR spectrum of POSS, provided in Supporting Information, is characterized by the T^2 and T^3 units, in which T^2 (−60.14 ppm) represents silanols and T^3 (−67.83 and −69.42 ppm) is assigned to cage siloxanes. The signals observed are similar to the values reported in literature at −58.6 (T^2), −67.9, and −68.4 (T^3) ppm.[49,50] Spectra were compared between sheared (thermally treated) and vortexed (ambient mixed) POSS-treated particle representative samples (M), and a decrease in intensity is observed for the silanol relative to cage siloxanes for sheared samples, supporting the IR results. Provided that the IR and NMR suggest that bonding between the particles and dispersant may have covalent character, a detailed study of the bonding in the POSS-treated particle samples was pursued using TGA. Particle modification was found to have a significant impact on thermal behavior of the correlating samples. TGA probes weight loss as a function of increasing temperature and is reported as a mass fraction. Powder composite samples were prepared under high shear as described previously and washed aggressively in hexane to eliminate loosely or nonbonded POSS. TGA was conducted on the washed and unwashed POSS-treated samples, M, N, and S, and reference TGA were obtained on the pure particle samples for comparison. In general, each powder sample contained 5−10 wt % of POSS to provide complete particle surface coverage, and representative plots of TGA data are provided in Figure 4. TGA plots of reference unmodified particles indicate the presence of adsorbed water at $T < 100$ °C, which is most pronounced in the silica sample and suggests larger water uptake from this solid under ambient conditions.

In a comparison of the washed and unwashed plots corresponding to the POSS-treated titania samples, Figure 4A,C, similar and interesting results present. Regardless of whether 5% or 10% of POSS is added to these samples, roughly 3% is strongly bound in the composite sample and resists removal by solvent washing. However, in the case of the silica sample, Figure 4B, virtually all of the added POSS is strongly

DOI: 10.1021/acsami.5b01488
ACS Appl. Mater. Interfaces 2015, 7, 12639−12648

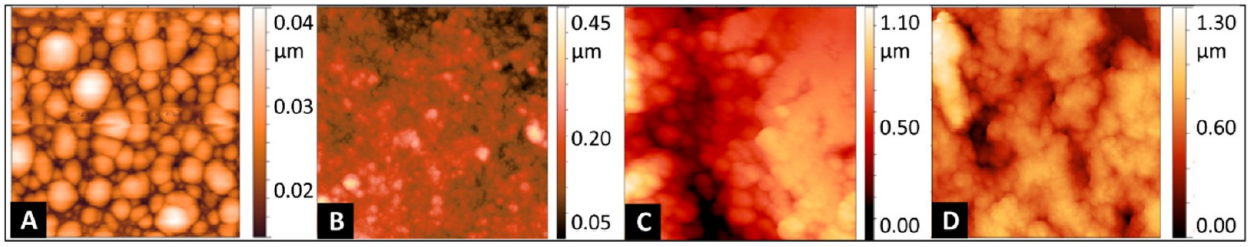

Figure 6. AFM topographic images of 10 × 10 μm^2 areas of coatings prepared from (A) TMPMP/TTT, (B) M/TMPMP/TTT, (C) S/TMPMP/TTT, (D) N/TMPMP/TTT. All samples were prepared from 2 wt % acetone dispersions, suitable for spray-coating, containing particle (1.6 wt %), dispersant (0.2 wt %), and thiol-ene monomers (0.2 wt %) except for sample A, which was prepared without particle or POSS.

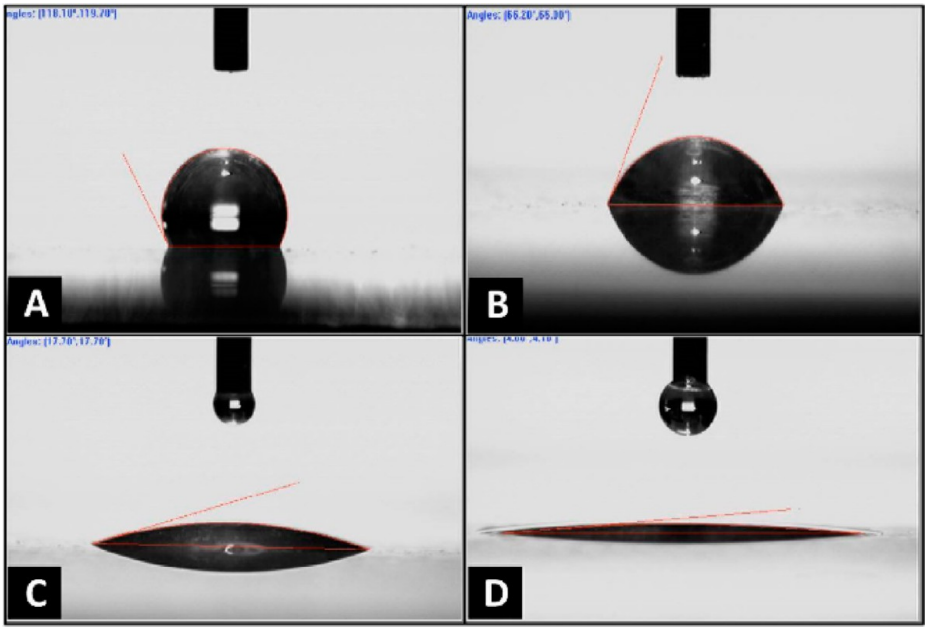

Figure 7. Illustration of the readily observable increase in surface wetting with exposure time of composite samples, M/TMPMP/TTT, T = 27 °C, λ_{max} = 350 nm: (A) t = 0 h, (B) t = 1 h, (C) t = 2 h, (D) t = 3 h.

bound to the surface, suggesting a higher efficiency for surface functionalization. Similar results were demonstrated recently by Wheeler et al.[29] in a study which included the preparation and characterization of a titania/POSS blend for dispersion in a polypropylene matrix.

The hydrophobic−hydrophilic transition in titania-containing films is shown to be heavily dependent upon the physical characteristics of the coating surface.[36,40−42] There is an optimal range of surface roughness, intermittent between smooth and obviously larger grain, that produces films possessing some microstructure and enhanced transition rates of hydrophobic−hydrophilic behavior. Sprayed films naturally produce interesting topologies, due to the nature of the application method. Solvent evaporation during application is likely a key contributor to film microstructure, along with the physical attributes of the dispersion, e.g., average particle size and the presence of dispersants. Titania-thiol-ene coatings were prepared on aluminum coupons from the monomer-containing dispersions using industry standard spray techniques and radiation cured to produce visually uniform films. The mechanical properties of the prepared composite films were evaluated using SEM, DSC, and AFM.

SEM was conducted to interrogate the coating topology and assess the results of the adhesion studies. In general, coatings were characterized by a uniform and heavily textured surface. A goal of this work is the incorporation of thiol-ene monomers designed to provide adhesion and mechanical strength to the composite photocatalytic coating. Since films prepared from the flexible ene composition, e.g., M/TMPMP/APE, were more easily marred through macroscopic mechanical etching, only those films prepared from the more rigid ene composition, e.g., M/TMPMP/TTT, were evaluated by adhesion tests and were selected as the preferred composition. Adhesion tests on prepared coatings were conducted using a standard crosshatch method ASTM D3359, and the coatings were evaluated after the adhesion test using SEM techniques. SEM inspection of residual coating material between hatch marks reveals that there is a significant improvement in adhesion via the incorporation of the polymer matrix. Example samples, imaged just after the adhesion test, reveal that less coating is removed in polymer networked samples, Figure 5.

Since we are attributing the mechanical integrity of the composite coating to the presence of the thiol-ene network created around the titania particle, a glass transition temperature (T_g) was acquired. The DSC plots of the thiol-ene network prepared using the preferred composition M/TMPMP/TTT and control samples TMPMP/TTT and POSS/TMPMP/TTT are included in the Supporting Information, Figure S7. The composite sample M/TMPMP/TTT is characterized by two transitions. The first transition, T_g,

DOI: 10.1021/acsami.5b01488
ACS Appl. Mater. Interfaces 2015, 7, 12639−12648

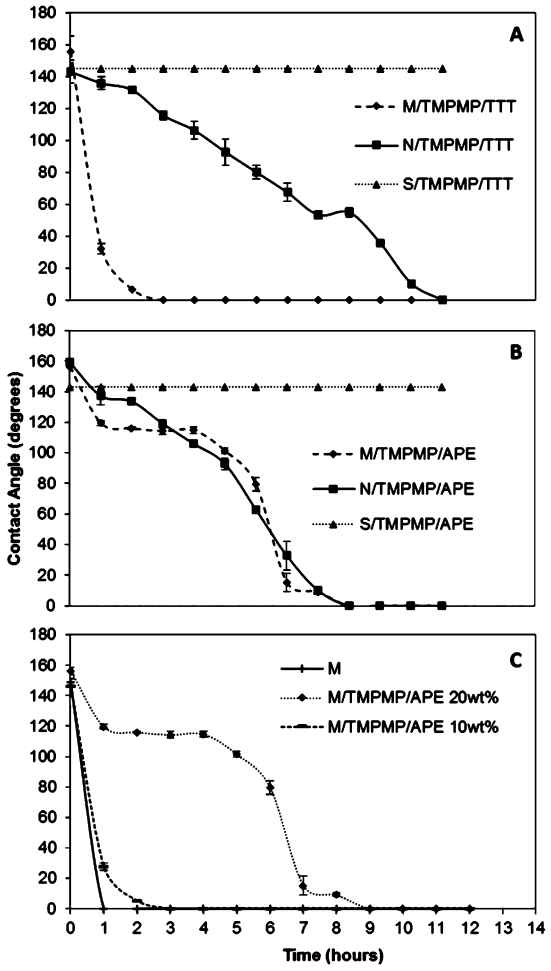

Figure 8. Change in static water contact angle measurements of POSS-containing M, S, and N composite coating series with increasing 350 nm exposure time (A) TMPMP/TTT, (b) TMPMP/APE, (c) TXMPMP/APE at 10 and 20 wt % monomer compositions with dispersed micron particle, M.

appears at a characteristic temperature for an inorganic-thiol-ene hybrid composite material, as described by recent literature.[51,52] A shift in the observed T_g at 37 °C from what is expected from the pure controls, polymer network TMPMP/TTT at 21 °C, and polymer plus POSS, POSS/TMPMP/TTT at 23 °C, is consistent with the significant doping by inorganic particle components. Our T_g value of 21 °C for the thiol-ene control TMPMP/TTT is comparable to the reported value of ~22 °C by Shin et al.[53] However, due to the large excess of photocatalytic titania relative to polymer, we attribute the second transition at approximately 49 °C to polymer material that has undergone enhanced cross-linking and other potential photodegradation reactions to produce a more rigid network at the particle surface. T_g's for the nanoscale materials, S and N polymer networks, were not readily resolved.

A topographic AFM analysis was conducted for each composite coating. In general, AFM results reinforce the rough surface suggested by SEM analysis, as displayed in Figure 6. Roughness values (RMS) were determined for the series, and M/TMPMP/TTT, N/TMPMP/TTT, and S/TMPMP/TTT yielded roughness values of 45.1, 239.0, and 217.0 nm. The thiol-ene control TMPMP/TTT yielded an RMS of 4.25 nm. It is important to note that SEM data covers a significantly larger area, which complicates a direct comparison. The spray method

Table 2. Change in Static Water Contact Angle with Continued Irradiation

sample name	λ (nm)	initial CA[a]	final CA	time (h)
M	313	>150	0	1
M	350	149.1	0	2
M/TMPMP/APE	313	159.1	8.7	4
M/TMPMP/APE	350	156.2	9.1	8
M/TMPMP/TTT	313	>150	0	1
M/TMPMP/TTT	350	155.5	5.5	2
N	313	>150	0	1
N	350	>150	6.8	2
N/TMPMP/APE	313	>150	7.8	4
N/TMPMP/APE	350	159.3	10.2	8
N/TMPMP/TTT	313	>150	10.3	5
N/TMPMP/TTT	350	143.1	10.4	11
S	313	155.2	131.4	36
S/TMPMP/APE	313	>150	>150	48[b]
S/TMPMP/TTT	313	>150	153.6	48[b]

[a]Where enhanced superhydrophobicity prevents the acquisition of a static contact angle measurement due to bead movement, a value of >150 is reported. [b]Indicates coating maintained superhydrophobic state after 48 h of continuous UV illumination; irradiation times of coatings applied to aluminum Q-panels; T = 27 °C; all samples were prepared from 2 wt % acetone dispersions, suitable for spray-coating, containing particle (1.6 wt %), dispersant (0.2 wt %), and thiol-ene monomers (0.2 wt %) except for samples M, N, and S, which were prepared without monomers for comparison.

of film application combined with a relatively volatile carrier phase may produce rough films on the submicrometer scale, which may be further enhanced by large particles or particle aggregates present in the dispersions. AFM results indicate that composite coatings N/TMPMP/TTT and S/TMPMP/TTT possessed larger features compared to the M/TMPMP/TTT coating. This was surprising since M is sold as a micron-scale particle, while S and N are nanoscale. TEM images supported the presence of large aggregates in N dispersions, which when combined with solvent evaporation during coating application could lead to the particle packing arrangements and cavernous topology observed. Although not as obvious in TEM analysis, perhaps a similar aggregation occurs in S samples, leading to comparable AFM images. A critical finding of this work is that although prepared using the same procedures, M-containing composite coatings are more uniform and less rough. Since a link has been established between surface microstructure and the hydrophobic−hydrophilic transition of photoactive coatings containing anatase titania, we probed the change in surface energy using water contact angles under continuous UV exposure.

A coated surface is considered wetted if a liquid spreads evenly over the surface without the formation of droplets and presents a contact angle <90°, implying that the surface interactions between the liquid and surface are stronger than the cohesive forces of bulk liquid. Conversely, a nonwetting surface is typically characterized by a contact angle >90°. When the solvent is water, the terms hydrophobic and hydrophilic are used to define these two wetting states. A more extreme scenario is the superhydrophobic and superhydrophilic conditions, which are characterized by water contact angles of >150° and <10°.[2,16]

All composite coatings prepared in this study presented superhydrophobic surfaces initially, and were characterized by high water contact angles. The transition from hydrophobic to

DOI: 10.1021/acsami.5b01488
ACS Appl. Mater. Interfaces 2015, 7, 12639−12648

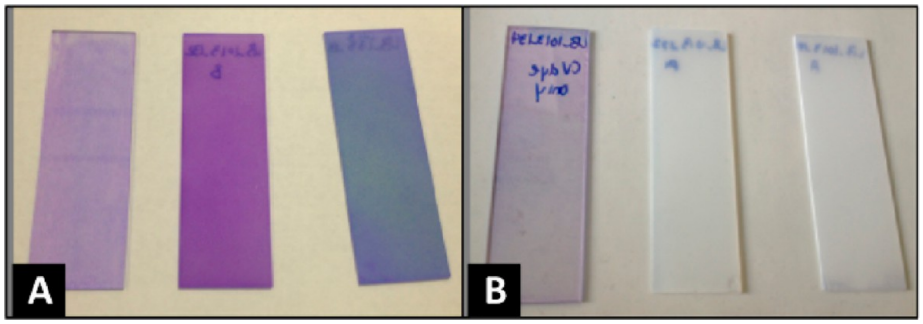

Figure 9. Representative samples illustrating photocatalytic degradation of crystal violet dye; from left to right: control (CV dye only), M, and M/TMPMP/TTT @ 20 wt % polymer (A) before UV exposure, T = 0, and (B) after UV exposure, T = 5 min.

hydrophilic surface was probed for composite coatings by taking time dependent water contact angles under continuous irradiation. An example progression from superhydrophobic to superhydrophilic of a M/TMPMP/APE coating is provided in Figure 7. Samples were placed in a custom environmentally controlled photoreactor sample chamber, irradiation at either 313 or 350 nm at a constant temperature and RH of 25 °C and 31 ± 2%, respectively. Samples were removed on the hour marks, and water contact angle obtained, until samples became superhydrophilic. Figure 8 illustrates the progression of surface characteristics of composite coatings from superhydrophobic to superhydrophilic. In all cases, the superhydrophobic character of silica-containing coatings persists over 48 h of continuous illumination.

In all cases, the coatings containing photocatalytic titania were converted to superhydrophilic surfaces. In many cases this conversion was complete within the first hour of exposure. Our composite coatings contain polymer to provide the "coating" characteristics of the composite, such as adhesion, cohesion, and mechanical integrity. In general, the presence of polymer delays the onset of superhydrophilicity, but does not prevent it. An increase in this induction time is noted as the polymer composition is increased, Figure 8C. As-produced coatings in many cases were so severely superhydrophobic that initial contact angles could not be obtained, since the water droplet preferred to adhere to the needle unless coaxed to fall, which resulted in the drop moving around on the surface and preventing the collection of a static contact angle. These points are denoted by a contact angle of >150 in Table 2.

The hydrophobic−hydrophilic transition of all particle−polymer combinations, M/TMPMP/APE, M/TMPMP/TTT, N/TMPMP/APE, N/TMPMP/TTT, S/TMPMP/APE, S/TMPMP/TTT, were exposed to continuous irradiation until superhydrophilic or 48 h. Several expected trends present. Hydrophobic−hydrophilic transitions occur more quickly at 313 nm, since a greater percentage of the photons exceed the band gap energy of the photocatalyst. The presence of polymers does not prohibit the transition, nor does the presence of monomer TTT seem to retard the transition appreciably more than APE despite its more competitive absorption characteristics. After coated panels reached a superhydrophilic state, samples were placed in a dark box to examine the rate at which the coatings regained their initial contact angles, i.e., returned to their hydrophobic state. Contact angles were obtained periodically until measurements were comparable to their values prior to irradiation. All coatings reverted to or maintained a hydrophobic state, greater than 90°, following 4−6 months of storage in complete darkness, 40−50% RH, and 27 °C. Given the slow rates of return, the superhydrophilic state is considered persistent with minimal light exposure. Similar to results obtained by Wynne and co-workers, where a surface energy switching composition of block polymers having hydrophilic and hydrophobic side chains was employed, the ability to tune surface interactions with the environment while maintaining good bulk mechanical properties and adhesion is of paramount importance to coatings applications.[54]

Anatase titania also serves as an effective photocatalyst for the degradation of organic pollutants.[55] In an effort to determine if the presence of the polymer additive will prohibit the photocatalytic activity, apart from the hydrophobic−hydrophilic transition, of the titania-containing composite coatings, the photocatalytic decomposition of crystal violet dye (pollutant proxy) was observed on controls with and without polymer, Figure 9.

Given that the photocatalytic degradation of surface-bound organics and the hydrophobic−hydrophilic transition is currently assumed to be synergistic,[56] we expected to observe the progression of the brightly colored crystal violet dye from purple to colorless upon irradiation. The M/TMPMP/TTT and POSS-treated M coatings were chosen as starting point compositions for comparison to pure crystal violet controls. Coatings were prepared as previously stated and exposed to UV light, 40−50% RH, and 27 °C for 2 h prior to the application of crystal violet dye. Via visual inspection, comparable color changes had occurred within 3 min for POSS-treated M coating and 30 min for the M/TMPMP/TTT coating, respectively. Similar to the hydrophobic−hydrophilic transition, the presence of polymer matrix retards the onset of photocatalytic activity, but does not prevent it. We are currently performing a detailed study into the rates and mechanisms of the photocatalytic degradation of crystal violet and other organic compounds of interest, including select chemical warfare agent stimulants, on our POSS-containing titania-thiol-ene composite photocatalytic coatings.

CONCLUSIONS

In summary, stable titania-thiol-ene dispersions at approximately 2 wt % solids were prepared using a combination of high-shear mixing and sonication in acetone solvent from photocatalytic anatase titania particles and trisilanol isobutyl polyhedral oligomeric silsesquioxane (POSS) dispersant. The presence of the POSS dispersant was critical to long-term dispersion stability. Interactions between the dispersant molecule and the particle surface were expected to vary from electrostatic to covalent in nature. Moreover, TGA and IR

DOI: 10.1021/acsami.5b01488
ACS Appl. Mater. Interfaces 2015, 7, 12639−12648

analysis supports that a portion of the molecular dispersant (roughly 3 wt %, wt/wt) is strongly bound to the particle surface, and this quantity is independent of the initial mass of dispersant added in the range 5−10 wt %. Although an initial concern, the addition of monomers to the dispersions does not promote agglomeration and samples retain the long term stability required for film preparation. Coatings were prepared from the dispersions using standard spray techniques to produce films having a uniform and heavily textured surface characterized via SEM and AFM analysis. In general, the presence of polymer matrix provided mechanical integrity of the coating, specifically adhesion, without significantly compromising or prohibiting other critical coating performance characteristics, such as film processing, photocatalytic degradation of adsorbed contaminants, and the hydrophobic−hydrophilic transition. In all cases, coatings containing photocatalytic titania were converted to superhydrophilic surfaces, whereas those that contained silica particles as reference materials remained superhydrophobic. The superhydrophilic state of samples was considered persistent, since long time durations in complete darkness were required to observe any significant hydrophobic return.

■ ASSOCIATED CONTENT

Supporting Information

Photoreactor and sample chamber design, light source emission spectra, DLS, FTIR, Si NMR, and DSC results. The Supporting Information is available free of charge on the ACS Publications website at DOI: 10.1021/acsami.5b01488.

■ AUTHOR INFORMATION

Corresponding Author

*Phone: (601) 266-4083. Fax: (601) 266-6075. E-mail: paige.buchanan@usm.edu.

Notes

The authors declare no competing financial interest.

■ ACKNOWLEDGMENTS

Financial support for this work was provided through the Department of Homeland Security Southeastern Region Research Initiative (SERRI), NSF GK-12 Program-University of Southern Mississippi, "Connections in the Classroom: Molecules to Muscles" Award 0947944, and the National Science Foundation CAREER Program Award CHE-0847481.

■ REFERENCES

(1) Fujishima, A.; Rao, T. N.; Tryk, D. A. Titanium Dioxide Photocatalysis. *J. Photochem. Photobiol., C* **2000**, *1*, 1−21.
(2) Fujishima, A.; Zhang, X.; Tryk, D. A. TiO_2 Photocatalysis and Related Surface Phenomena. *Surf. Sci. Rep.* **2008**, *63*, 515−582.
(3) Henderson, M. A. A Surface Science Perspective on Photocatalysis. *Surf. Sci. Rep.* **2011**, *66*, 185−297.
(4) Herrmann, J.-M. Heterogeneous Photocatalysis: Fundamentals and Applications to the Removal of Various Types of Aqueous Pollutants. *Catal. Today* **1999**, *53*, 115−129.
(5) Fox, M. A.; Dulay, M. T. Heterogeneous Photocatalysis. *Chem. Rev.* **1993**, *93*, 341−357.
(6) Chen, X.; Mao, S. S. Titanium Dioxide Nanomaterials: Synthesis, Properties, Modifications, and Applications. *Chem. Rev.* **2007**, *107*, 2891−2959.
(7) Guan, K. Relationship between Photocatalytic Activity, Hydrophilicity and Self-Cleaning Effect of TiO_2/ SiO_2 Films. *Surf. Coat. Technol.* **2005**, *191*, 155−160.
(8) Demeestere, K.; Dewulf, J.; Van Langenhove, H. Heterogeneous Photocatalysis as an Advanced Oxidation Process for the Abatement of Chlorinated, Monocyclic Aromatic and Sulfurous Volatile Organic Compounds in Air: State of the Art. *Crit. Rev. Environ. Sci. Technol.* **2007**, *37*, 489−538.
(9) Hoffmann, M. R.; Martin, S. T.; Choi, W.; Bahnemann, D. W. Environmental Applications of Semiconductor Photocatalysis. *Chem. Rev.* **1995**, *95*, 69−96.
(10) Fujishima, A.; Zhang, X.; Tryk, D. A. Heterogeneous Photocatalysis: From Water Photolysis to Applications in Environmental Cleanup. *Int. J. Hydrogen Energy* **2007**, *32*, 2664−2672.
(11) Diebold, U. The Surface Science of Titanium Dioxide. *Surf. Sci. Rep.* **2003**, *48*, 53−229.
(12) Kazuhito, H.; Hiroshi, I.; Akira, F. TiO_2 Photocatalysis: A Historical Overview and Future Prospects. *Jpn. J. Appl. Phys.* **2005**, *44*, 8269−8285.
(13) Sirghi, L.; Hatanaka, Y. Hydrophilicity of Amorphous TiO_2 Ultra-Thin Films. *Surf. Sci.* **2003**, *530*, L323−L327.
(14) Wang, S.; Song, Y.; Jiang, L. Photoresponsive Surfaces with Controllable Wettability. *J. Photochem. Photobiol., C* **2007**, *8*, 18−29.
(15) White, J. M.; Szanyi, J.; Henderson, M. A. The Photon-Driven Hydrophilicity of Titania: A Model Study Using TiO_2 (110) and Adsorbed Trimethyl Acetate. *J. Phys. Chem. B* **2003**, *107*, 9029−9033.
(16) Verplanck, N.; Coffinier, Y.; Thomy, V.; Boukherroub, R. Wettability Switching Techniques on Superhydrophobic Surfaces. *Nanoscale Res. Lett.* **2007**, *2*, 577−596.
(17) Miyauchi, M.; Kieda, N.; Hishita, S.; Mitsuhashi, T.; Nakajima, A.; Watanabe, T.; Hashimoto, K. Reversible Wettability Control of TiO_2 Surface by Light Irradiation. *Surf. Sci.* **2002**, *511*, 401−407.
(18) Veronovski, N.; Andreozzi, P.; La Mesa, C.; Sfiligoj-Smole, M. Stable TiO_2 Dispersions for Nanocoating Preparation. *Surf. Coat. Technol.* **2010**, *204*, 1445−1451.
(19) Siti Hajar, O.; Suraya Abdul, R.; Tinia Idaty Mohd, G.; Norhafizah, A. Dispersion and Stabilization of Photocatalytic TiO_2 Nanoparticles in Aqueous Suspension for Coatings Applications. *J. Nanomater.* **2012**, *2012*, 1−10.
(20) Magdalena, N.; Damian, A. e.; Teofil, J. TiO_2-SiO_2/Ph-POSS Functional Hybrids: Preparation and Characterisation. *J. Nanomater.* **2013**, *2013*, 1−10.
(21) Wu, J.; Mather, P. T. POSS Polymers: Physical Properties and Biomaterials Applications. *Polym. Rev.* **2009**, *49*, 25−63.
(22) Ambrozewicz, D.; Marciniec, B.; Jesionowski, T. New POSS/Magnesium Silicate Nano-Hybrids Obtained by Chemical or Mechanical Methods. *Chem. Eng. J.* **2012**, *210*, 229−236.
(23) Nowacka, M.; Siwinska-Stefanska, K.; Jesionowski, T. Structural Characterisation of Titania or Silane-Grafted TiO_2-SiO_2 Oxide Composite and Influence of Ionic Strength or Electrolyte Type on Their Electrokinetic Properties. *Colloid Polym. Sci.* **2013**, *291*, 603−612.
(24) Cook, R. D.; Wheeler, P. A.; Misra, R. Nanoparticle Dispersion Utilizing Polyhedral Oligomeric Silsesquioxane. *Polym. Prepr.* **2007**, *48*, 449−450.
(25) Lickiss, P. D.; Rataboul, F. Fully Condensed Polyhedral Oligosilsesquioxanes (POSS): From Synthesis to Application. *Adv. Organomet. Chem.* **2008**, *57*, 1−116.
(26) Lee, A.; Lichtenhan, J. D. Viscoelastic Responses of Polyhedral Oligosilsesquioxane Reinforced Epoxy Systems. *Macromolecules* **1998**, *31*, 4970−4974.
(27) Szwarc-Rzepka, K.; Marciniec, B.; Jesionowski, T. Immobilization of Multifunctional Silsesquioxane Cage on Precipitated Silica Supports. *Adsorption* **2013**, *19*, 483−494.
(28) Szwarc-Rzepka, K.; Ciesielczyk, F.; Jesionowski, T. Preparation and Physicochemical Properties of Functionalized Silica/Octamethacryl-Silsesquioxane Hybrid Systems. *J. Nanomater.* **2013**, *2013*, 1−15.
(29) Wheeler, P. A.; Misra, R.; Cook, R. D.; Morgan, S. E. Polyhedral Oligomeric Silsesquioxane Trisilanols as Dispersants for Titanium Oxide Nanopowder. *J. Appl. Polym. Sci.* **2008**, *108*, 2503−2508.

DOI: 10.1021/acsami.5b01488
ACS Appl. Mater. Interfaces 2015, 7, 12639−12648

(30) Lowe, A. B. Thiol-Ene "Click" Reactions and Recent Applications in Polymer and Materials Synthesis. *Polym. Chem.* **2010**, *1*, 17−36.
(31) Hoyle, C. E.; Bowman, C. N. Thiol−Ene Click Chemistry. *Angew. Chem., Int. Ed.* **2010**, *49*, 1540−1573.
(32) Hoyle, C. E.; Lowe, A. B.; Bowman, C. N. Thiol-Click Chemistry: A Multifaceted Toolbox for Small Molecule and Polymer Synthesis. *Chem. Soc. Rev.* **2010**, *39*, 1355−1387.
(33) Tucker-Schwartz, A. K.; Farrell, R. A.; Garrell, R. L. Thiol-Ene Click Reaction as a General Route to Functional Trialkoxysilanes for Surface Coating Applications. *J. Am. Chem. Soc.* **2011**, *133*, 11026−11029.
(34) Phillips, J. P.; Mackey, N. M.; Confait, B. S.; Heaps, D. T.; Deng, X.; Todd, M. L.; Stevenson, S.; Zhou, H.; Hoyle, C. E. Dispersion of Gold Nanoparticles in UV-Cured, Thiol-Ene Films by Precomplexation of Gold-Thiol. *Chem. Mater.* **2008**, *20*, 5240−5245.
(35) Andrew, M.; Matthew, C. A Study of Factors That Change the Wettability of Titania Films. *Int. J. Photoenergy* **2008**, *2008*, 1−6.
(36) Arimitsu, N.; Nakajima, A.; Katsumata, K.-i.; Shiota, T.; Watanabe, T.; Yoshida, N.; Kameshima, Y.; Okada, K. Photoinduced Surface Roughness Variation in Polycrystalline TiO_2 Thin Films under Different Atmospheres. *J. Photochem. Photobiol., A* **2007**, *190*, 53−57.
(37) Fateh, R.; Dillert, R.; Bahnemann, D. Self-Cleaning Properties, Mechanical Stability, and Adhesion Strength of Transparent Photocatalytic TiO_2-ZnO Coatings on Polycarbonate. *ACS Appl. Mater. Interfaces* **2014**, *6*, 2270−2278.
(38) Guan, K.; Lu, B.; Yin, Y. Enhanced Effect and Mechanism of SiO_2 Addition in Super-Hydrophilic Property of TiO_2 Films. *Surf. Coat. Technol.* **2003**, *173*, 219−223.
(39) Hwang, Y. K.; Patil, K. R.; Kim, H.-K.; Sathaye, S. D.; Hwang, J.-S.; Park, S.-E.; Chang, J.-S. Photoinduced Superhydrophilicity in TiO_2 Thin Films Modified with WO_3. *Bull. Korean Chem. Soc.* **2005**, *26*, 1515−1519.
(40) Katsumata, K.-i.; Nakajima, A.; Yoshikawa, H.; Shiota, T.; Yoshida, N.; Watanabe, T.; Kameshima, Y.; Okada, K. Effect of Microstructure on Photoinduced Hydrophilicity of Transparent Anatase Thin Films. *Surf. Sci.* **2005**, *579*, 123−130.
(41) Law, W. S.; Lam, S. W.; Gan, W. Y.; Scott, J.; Amal, R. Effect of Film Thickness and Agglomerate Size on the Superwetting and Fog-Free Characteristics of TiO_2 Films. *Thin Solid Films* **2009**, *517*, 5425−5430.
(42) Miyauchi, M.; Kieda, N.; Hishita, S.; Mitsuhashi, T.; Nakajima, A.; Watanabe, T.; Hashimoto, K. Reversible Wettability Control of TiO_2 Surface by Light Irradiation. *Surf. Sci.* **2002**, *511*, 401−407.
(43) Miyauchi, M.; Nakajima, A.; Watanabe, T.; Hashimoto, K. Photocatalysis and Photoinduced Hydrophilicity of Various Metal Oxide Thin Films. *Chem. Mater.* **2002**, *14*, 2812−2816.
(44) Sahoo, M.; Mathews, T.; Antony, R. P.; Krishna, D. N.; Dash, S.; Tyagi, A. K. Physicochemical Processes and Kinetics of Sunlight-Induced Hydrophobic↔Superhydrophilic Switching of Transparent N-Doped TiO_2 Thin Films. *ACS Appl. Mater. Interfaces* **2013**, *5*, 3967−3974.
(45) Stevens, N.; Priest, C. I.; Sedev, R.; Ralston, J. Wettability of Photoresponsive Titanium Dioxide Surfaces. *Langmuir* **2003**, *19*, 3272−3275.
(46) Sun, R.-D.; Nakajima, A.; Fujishima, A.; Watanabe, T.; Hashimoto, K. Photoinduced Surface Wettability Conversion of ZnO and TiO_2 Thin Films. *J. Phys. Chem. B* **2001**, *105*, 1984−1990.
(47) Xi, B.; Verma, L. K.; Li, J.; Bhatia, C. S.; Danner, A. J.; Yang, H.; Zeng, H. C. TiO_2 Thin Films Prepared Via Adsorptive Self-Assembly for Self-Cleaning Applications. *ACS Appl. Mater. Interfaces* **2012**, *4*, 1093−1102.
(48) Godnjavec, J.; Znoj, B.; Veronovski, N.; Venturini, P. Polyhedral Oligomeric Silsesquioxanes as Titanium Dioxide Surface Modifiers for Transparent Acrylic UV Blocking Hybrid Coating. *Prog. Org. Coat.* **2012**, *74*, 654−659.
(49) Jerman, I.; Kozelj, M.; Orel, B. The Effect of Polyhedral Oligomeric Silsesquioxane Dispersant and Low Surface Energy Additives on Spectrally Selective Paint Coatings with Self-Cleaning Properties. *Sol. Energy Mater. Sol. Cells* **2010**, *94*, 232−245.
(50) Ashu-Arrah, B. A.; Glennon, J. D.; Albert, K. Spectroscopic and Chromatographic Characterisation of a Pentafluorophenylpropyl Silica Phase End-Capped in Supercritical Carbon Dioxide as a Reaction Solvent. *J. Chromatogr. A* **2013**, *1298*, 86−94.
(51) Sangermano, M.; Gross, S.; Priola, A.; Rizza, G.; Sada, C. Thiol-Ene Hybrid Organic/Inorganic Nanostructured Coatings Based on Thiol-Functionalized Zirconium Oxoclusters. *Macromol. Chem. Phys.* **2007**, *208*, 2560−2568.
(52) Schreck, K. M.; Leung, D.; Bowman, C. N. Hybrid Organic/Inorganic Thiol-Ene-Based Photopolymerized Networks. *Macromolecules* **2011**, *44*, 7520−7529.
(53) Shin, J.; Nazarenko, S.; Hoyle, C. E. Enthalpy Relaxation of Photopolymerized Thiol−Ene Networks: Structural Effects. *Macromolecules* **2008**, *41*, 6741−6746.
(54) Zhang, W.; Fujiwara, T.; Taşkent, H.; Zheng, Y.; Brunson, K.; Gamble, L.; Wynne, K. J. A Polyurethane Surface Modifier: Contrasting Amphiphilic and Contraphilic Surfaces Driven by Block and Random Soft Blocks Having Trifluoroethoxymethyl and Peg Side Chains. *Macromol. Chem. Phys.* **2012**, *213*, 1415−1434.
(55) Wang, S.; Ang, H. M.; Tade, M. O. Volatile Organic Compounds in Indoor Environment and Photocatalytic Oxidation: State of the Art. *Environ. Int.* **2007**, *33*, 694−705.
(56) Huang, T.; Huang, W.; Zhou, C.; Situ, Y.; Huang, H. Superhydrophilicity of TiO_2/ SiO_2 Thin Films: Synergistic Effect of SiO_2 and Phase-Separation-Induced Porous Structure. *Surf. Coat. Technol.* **2012**, *213*, 126−132.

DOI: 10.1021/acsami.5b01488
ACS Appl. Mater. Interfaces 2015, 7, 12639−12648